UCSF
UC San Francisco Previously Published Works

Title

A single dose of peripherally infused EGFRvIII-directed CAR T cells mediates antigen loss and induces adaptive resistance in patients with recurrent glioblastoma

Permalink

https://escholarship.org/uc/item/6x8957wx

Journal

Science Translational Medicine, 9(399)

ISSN

1946-6234

Authors

O'Rourke, Donald M
Nasrallah, MacLean P
Desai, Arati
et al.

Publication Date

2017-07-19

DOI

10.1126/scitranslmed.aaa0984

Peer reviewed

A single dose of peripherally infused EGFRvIII-directed CAR T cells mediates antigen loss and induces adaptive resistance in patients with recurrent glioblastoma

Donald M. O'Rourke[1], MacLean P. Nasrallah[2,*], Arati Desai[3,*], Jan J. Melenhorst[4,*], Keith Mansfield[5,*], Jennifer J. D. Morrissette[6], Maria Martinez-Lage[2,†], Steven Brem[1], Eileen Maloney[1], Angela Shen[7], Randi Isaacs[5], Suyash Mohan[8], Gabriela Plesa[4], Simon F. Lacey[4], Jean-Marc Navenot[4], Zhaohui Zheng[4], Bruce L. Levine[4], Hideho Okada[9], Carl H. June[4], Jennifer L. Brogdon[5], and Marcela V. Maus[10,‡]

[1]Department of Neurosurgery, Perelman School of Medicine at the University of Pennsylvania, Philadelphia, PA 19104, USA

[2]Division of Neuropathology, Department of Pathology and Laboratory Medicine, Perelman School of Medicine at the University of Pennsylvania, Philadelphia, PA 19104, USA

[3]Department of Medicine, Perelman School of Medicine at the University of Pennsylvania, Philadelphia, PA 19104, USA

[4]Center for Cellular Immunotherapies, University of Pennsylvania, Philadelphia, PA 19104, USA

[5]Novartis Institutes for BioMedical Research, Cambridge, MA 02139, USA

[6]Division of Precision and Computational Diagnostics, Department of Pathology and Laboratory Medicine, Perelman School of Medicine at the University of Pennsylvania, Philadelphia, PA 19104, USA

[7]Novartis Oncology, East Hanover, NJ 07936, USA

[8]Division of Neuroradiology, Department of Radiology, Perelman School of Medicine at the University of Pennsylvania, Philadelphia, PA 19104, USA

[9]Department of Neurosurgery, University of California, San Francisco, San Francisco, CA 94143, USA

‡Corresponding author. mvmaus@mgh.harvard.edu.
†Present address: Department of Pathology, Massachusetts General Hospital, Boston, MA 02114, USA.
*These authors contributed equally to this work.

[10]Cellular Immunotherapy Program, Cancer Center and Department of Medicine, Massachusetts General Hospital, Boston, MA 02129, USA

Abstract

We conducted a first-in-human study of intravenous delivery of a single dose of autologous T cells redirected to the epidermal growth factor receptor variant III (EGFRvIII) mutation by a chimeric antigen receptor (CAR). We report our findings on the first 10 recurrent glioblastoma (GBM) patients treated. We found that manufacturing and infusion of CAR-modified T cell (CART)–EGFRvIII cells are feasible and safe, without evidence of off-tumor toxicity or cytokine release syndrome. One patient has had residual stable disease for over 18 months of follow-up. All patients demonstrated detectable transient expansion of CART-EGFRvIII cells in peripheral blood. Seven patients had post–CART-EGFRvIII surgical intervention, which allowed for tissue-specific analysis of CART-EGFRvIII trafficking to the tumor, phenotyping of tumor-infiltrating T cells and the tumor microenvironment in situ, and analysis of post-therapy EGFRvIII target antigen expression. Imaging findings after CART immunotherapy were complex to interpret, further reinforcing the need for pathologic sampling in infused patients. We found trafficking of CART-EGFRvIII cells to regions of active GBM, with antigen decrease in five of these seven patients. In situ evaluation of the tumor environment demonstrated increased and robust expression of inhibitory molecules and infiltration by regulatory T cells after CART-EGFRvIII infusion, compared to pre–CART-EGFRvIII infusion tumor specimens. Our initial experience with CAR T cells in recurrent GBM suggests that although intravenous infusion results in on-target activity in the brain, overcoming the adaptive changes in the local tumor microenvironment and addressing the antigen heterogeneity may improve the efficacy of EGFRvIII-directed strategies in GBM.

INTRODUCTION

Malignant gliomas are the most common type of primary brain tumors, with glioblastoma (GBM) being the most common and most malignant of the glial tumors. No current treatment is curative because these tumors are invasive and grow aggressively in the central nervous system (CNS). No significant advancements in the treatment of GBM have occurred in the past 25 years except for temozolomide chemotherapy combined with radiotherapy, which demonstrated a limited prolongation of survival (1). Novel antiangiogenic agents (2, 3) and a variety of targeted kinase inhibitors (4) may be of limited efficacy when used as monotherapy. Median survival for newly diagnosed GBM is still less than 2 years (5). Even with standard-of-care therapy with chemoradiation and adjuvant temozolomide, GBM patients with significant residual disease after surgery have an average survival that is on the order of 6 months, with even poorer survival observed when the disease recurs in a multifocal fashion (1, 6). GBM tumors with un-methylated O^6-methylguanine methyltransferase (MGMT), a DNA repair enzyme, are also more resistant to radiation and temozolomide (7, 8), making unmethylated MGMT a poor prognostic marker.

Epidermal growth factor receptor (EGFR) variant III (EGFRvIII) is the most common variant of the EGFR observed in human tumors (9). It results from the in-frame deletion of exons 2 to 7 and the generation of a novel glycine residue at the junction of exons 1 and 8. This novel juxtaposition of amino acids within the extracellular domain of the EGFR creates

a tumor-specific, oncogenic, and immunogenic epitope. EGFRvIII is expressed in about 30% of newly diagnosed GBM cases (10), and in patients surviving a year or longer, the expression of EGFRvIII is thought to be a negative prognostic indicator, regardless of other factors such as extent of resection and age (11–13), perhaps in part because its oncogenic properties confer increased stability and sustained tumorigenic signaling (14). One therapeutic approach has been the targeting of the EGFRvIII mutant oncoprotein with a peptide vaccine strategy (rindopepimut). In phase 2 studies, rindopepimut was well tolerated and immune responses were observed (15); however, antigen escape variants have been noted (16), indicating that EGFRvIII may not be a sole driver mutation or otherwise necessary to maintain the tumorigenic phenotype.

Adoptive immunotherapy with redirected T cells obviates the need for antigen presentation and stimulation of a primary immune response and is potentially more effective and could have more favorable kinetics compared to vaccines. T cells redirected with chimeric antigen receptors (CARs) targeting the B cell marker CD19 have shown marked and durable efficacy in acute lymphoblastic leukemia, chronic lymphocytic leukemia, and B cell lymphomas (17–20). CAR T cells directed to solid tumors have not demonstrated efficacy as frequently (21–23), but in a recent report, genetically modified T cells directed to the interleukin-13 (IL-13) receptor α2 and infused multiple times intratumorally and intrathecally induced complete regression of metastatic GBM in one patient (24). We recently generated a CAR directed to EGFRvIII and described its target specificity, functional properties, and efficacy against EGFRvIII-expressing tumor cells in vitro and in xenogeneic mouse models (25, 26). We now report on the results of our first-in-human clinical trial of CAR-modified T cell (CART)–EGFRvIII in patients with recurrent GBM expressing EGFRvIII.

RESULTS

Clinical protocol design

We opened a phase 1 study (NCT02209376) to evaluate the feasibility and safety of manufacturing and administering CART-EGFRvIII cells to patients with EGFRvIII-expressing recurrent GBM. Patients with newly diagnosed or recurrent GBM referred to or treated at the University of Pennsylvania were offered testing of their tumor for expression of the EGFRvIII mutation by a validated RNA-based next-generation sequencing (NGS) assay; an antibody to test EGFRvIII expression by immunohistochemistry is desirable but was not available. Testing for EGFRvIII expression could be performed as a standard-of-care assay or as part of the screening procedures for enrollment on this clinical protocol. Patients were considered to have positive EGFRvIII expression if their tumors expressed EGFRvIII with a minimum of 100 reads. EGFRvIII percentage was calculated as (EGFRvIII reads)/[wild-type (WT) EGFR reads + EGFRvIII reads]. First preference was given to those with greater than 30% EGFRvIII, but in cases with extensive wild-type EGFR amplification, individuals with tumors containing as low as 6% EGFRvIII were considered eligible. In cases where patients had had previous EGFRvIII-directed therapy (such as rindopepimut), EGFRvIII expression had to be confirmed after recurrence to avoid treating patients whose tumors had already lost EGFRvIII expression. Additional eligibility criteria included adequate organ function and performance status and a histopathologic diagnosis of GBM.

Written informed consent was obtained for leukapheresis and treatment in two separate steps. Determination of EGFRvIII-expressing GBM was required for leukapheresis on the first step (step 1) of this protocol; evidence of recurrent or progressive disease triggered manufacturing of the CART-EGFRvIII product (Fig. 1A). Upon enrollment on the treatment phase (step 2) of the protocol, subjects underwent baseline magnetic resonance imaging (MRI), and their CART-EGFRvIII product was infused within 1 week (on day 0). The primary end points of the trial were safety and feasibility, and the secondary end points included response rate and overall survival. Correlative studies included measurement of expansion and persistence of CART-EGFRvIII cells by quantitative polymerase chain reaction (qPCR) and flow cytometry and cytokine release associated with infusion of CART-EGFRvIII cells. The study was opened after obtaining national and local regulatory approvals.

Over the course of 2 years, tumor specimens from 369 patients with histologically confirmed GBM were tested for EGFRvIII at our institution as standard of care using the NGS assay. Of these, 79 (21%) tested positive for EGFRvIII. The protocol completed accrual in less than 20 months. In that time, 17 patients whose tumors had tested positive for EGFRvIII were consented for leukapheresis and underwent initial screening on step 1 of the protocol (Fig. 1B). Of these, three had clinical decline before proceeding to leukapheresis. Fourteen subjects had their T cells collected by leukapheresis; one subject was subsequently withdrawn from the study by the investigator (due to rapid decline just before infusion), and three subjects (all with MGMT promoter–methylated GBM, which portends a better prognosis and responsiveness to standard chemotherapy) had not yet progressed to enroll on the treatment step of the protocol. Ten subjects have been infused with CART-EGFRvIII cell products.

Neurosurgical intervention in CART-EGFRvIII–infused patients—The original protocol design had an initial response assessment 1 month after CART-EGFRvIII infusion. In the first five subjects, the 1-month MRI was interpreted as stable disease by RANO (Response Assessment in Neuro-Oncology) criteria; one patient (207) had evidence of progression on MRI. However, after infusion of the first three subjects on this study and recognizing the complexity of the MRI findings and their interpretation, particularly in the context of an immunotherapy, we focused the study on understanding CART-EGFRvIII cell trafficking to the brain and their effects in the tumor. Unfortunately, there are no currently available clinical methods to directly image CART-EGFRvIII cell trafficking in the brain, making it impossible to noninvasively measure in situ CART-EGFRvIII pharmacokinetics or pharmacodynamics. Neurosurgical intervention was not obligatory as part of the original protocol design or an end point of this study but was clinically indicated at some point during the course of post-CART infusion treatment in seven patients. The timing of neurosurgical intervention was based on imaging findings suggestive of disease progression, as determined by the clinical and neuroradiology teams. Overall, there were three groups of subjects: (i) those who did not undergo surgery after CART infusion (the first three subjects treated in this study, all of whom had multifocal and/or deep-seated recurrence not amenable to surgical resection before CART infusion), (ii) those who underwent "late surgery" for presumed recurrence based on radiographic imaging after CART infusion (the second group

of three subjects treated who had surgery once at either day 34, day 55, or day 104 after CART-EGFRvIII infusion), and (iii) those who underwent "early surgery" in whom it was determined that surgery was indicated because of clear symptomatic progression. In this latter subgroup of four subjects, the CART product had been manufactured before clinical decline, and we therefore determined that surgery after CART infusion would provide an opportunity to evaluate CART-EGFRvIII biology without a delay in clinical intervention. This early surgery subgroup enabled the evaluation of the kinetics of early CART-EGFRvIII trafficking and alteration of the tumor microenvironment in GBM. The late surgery group allowed for the opportunity to evaluate the duration of CART-EGFRvIII persistence and potential activity in the tumor. Although the patients who underwent early surgery were not evaluable for radiographic response or progression-free survival assessments relative to CART-EGFRvIII infusion, the surgical procedures provided the only direct opportunity to evaluate the biology of adoptive T cell transfer across the blood-brain barrier in human patients with GBM.

Clinical results

Study subjects—The patient characteristics, level of EGFRvIII expression, and CART-EGFRvIII dose received are shown in summary form in Table 1. The characteristics of individual patients are shown in table S1, and individual product and dose characteristics are shown in table S2. The ages ranged from 45 to 76 years, and 50% of the subjects were male. The median time from diagnosis to infusion was 358 days, with a range of 179 to 682 days. Of the 10 subjects infused, 2 were treated with CART-EGFRvIII as their second line of treatment (that is, with evidence of progressive disease after completion of first-line standard treatment with surgery, chemoradiation, and one or more cycles of adjuvant temozolomide). Four were treated with CART-EGFRvIII as third-line treatment, and four were treated with CART-EGFRvIII as fourth-line treatment. Previous second- and third-line treatments included surgery, bevacizumab, chemotherapy (CCNU and/or carboplatin and/or lomustine), or dendritic cell vaccine. The details of each patient's age, time from initial diagnosis, performance status, steroid dose, EGFRvIII expression levels, and previous treatments are described in table S1. Nine of the 10 subjects had multifocal disease, a group of patients who are often excluded from other clinical trials because of poor prognosis; the 10th subject had a deep-seated multilobulated GBM involving the thalamus and midbrain that was not amenable to complete surgical resection and is uniformly associated with poor prognosis. All subjects had GBM with unmethylated MGMT promoter at some point in the course of their disease, a poor prognostic indicator (27). Karnofsky performance status ranged from 60 to 100%, with most subjects in the 80 to 90% range at infusion. Subjects were allowed to maintain a limited and stable dose of concurrent dexamethasone of up to 4 mg daily, but efforts were made to wean patients from steroids when clinically feasible, so as to avoid suppression of the CAR T cells; two patients were receiving steroids at the time of CART-EGFRvIII infusion. The median level of expression of EGFRvIII was 71% and ranged from 6% (in a subject with extensive amplification of wild-type EGFR) to 96%. Despite previous treatment with temozolomide and radiation, all subjects had successful manufacturing of their CART-EGFRvIII cell product. The CART-EGFRvIII product is composed of autologous T cells transduced with a lentiviral vector coding for a CAR that binds to EGFRvIII with a humanized single-chain variable fragment and signals using CD3ζ and the

4-1BB costimulation domain, which we previously described (26). The product was manufactured using our established methods to stimulate, transduce, and formulate the CAR T cells for intravenous infusion (28–30). The median transduction efficiency of 19.75% met the target dose of 1×10^8 to 5×10^8 CART-EGFRvIII⁺ and all other release criteria (Table 1). The transduction efficiency and exact dose are described for each patient in table S2.

Safety—As a phase 1 trial, the primary end point of this study was safety. The individual and significant post-CART infusion events and treatments are described and listed in table S3. All adverse events considered by the principal investigator to be related to CART-EGFRvIII cells are listed in table S4. The adverse events of special interest were considered to be (i) evidence of off-target toxicity related to EGFR, (ii) systemic cytokine release syndrome (characterized by fever, hypotension, and elevated inflammatory markers), and (iii) neurologic changes. No subjects experienced evidence of EGFR-directed toxicity (such as rash, diarrhea, or pulmonary symptoms) or systemic cytokine release syndrome. Three subjects experienced clinically significant neurologic events, which are common in this population because of the nature of the disease but could also be related to CART-EGFRvIII–induced immune responses in the confined intracranial space. One subject (202) had a seizure at day 9, followed by several days of altered mental status. The etiology of the seizure was unclear, because the patient also had viable GBM and hyponatremia. In addition to high-dose steroids and antiepileptics, this subject was treated with siltuximab (anti–IL-6) at day 15 in an effort to treat hypothesized "intracranial" cytokine release; the subject recovered to his baseline mental status over several days, but the recovery could not be attributed to a single intervention. A second patient (211) had neurologic decline at day 15 and was treated with high-dose steroids followed by siltuximab at day 29, but the overall clinical assessment was more consistent with progressive disease. A third patient (213) experienced neurologic decline in the postoperative setting, which was attributed to delayed hemorrhage in the operative bed that required clinical observation but not repeat surgical intervention. In summary, there were no dose-limiting toxicities, and CART-EGFRvIII was not associated with EGFR-directed toxicity, systemic cytokine release syndrome, or the neurotoxicity signs and symptoms observed with CD19-directed immunotherapy (31–33). However, neurologic effects such as seizures could be related to disease or localized T cell activation with an intracranial compartmentalized cytokine release.

Clinical end points

All subjects' tumors were assessed by MRI per protocol and clinical standards. Subjects remained on this study until clear disease progression or initiation of other medical treatments and then were followed on a long-term follow-up study as mandated by the U.S. Food and Drug Administration (FDA) for subjects receiving genetically modified products. Duration of follow-up while on study and duration of follow-up off study are indicated in Fig. 1C. Asterisks indicate the timing of neurosurgical intervention, which, in one subject (207), coincided with clear progression and removal from study. One patient remains alive and well without further therapy for more than 18 months after a single infusion of CART-EGFRvIII (subject 209). Two other subjects are alive but have clearly progressed by imaging criteria. A Kaplan-Meier plot of overall survival (OS) is shown (Fig. 1D), with median OS

of 251 days (~8 months) in these 10 subjects. Progression-free survival was not evaluable because of the confounding factor of neurosurgical intervention in most of the subjects.

Peripheral blood engraftment and persistence of CART-EGFRvIII

We detected CART-EGFRvIII cells in all infused subjects by qPCR analysis and flow cytometric analysis of peripheral blood mono-nuclear cells (PBMCs). The ability to detect infused CAR T cells has been defined as engraftment (34), although it does not necessarily define a duration. CAR gene marking via qPCR analysis was quantified relative to genomic DNA as described (28). CART-EGFRvIII cells were quantified as percent staining with soluble bis-biotinylated EGFRvIII of the gated T cell population (fig. S1); this reagent, a soluble version of the extracellular domain of soluble EGFRvIII, was extensively validated in preclinical and translational studies (26). All subjects infused had detectable circulating CART-EGFRvIII cells in the first month after infusion. The peak expansion occurred between days 3 and 10 in all subjects. Patient 202 received high-dose dexamethasone at day 9, and a transient decrease in CART-EGFRvIII in the peripheral blood was noted by both flow cytometry and qPCR. No lymphodepleting chemotherapy was administered to the subjects, but several of them were lymphopenic at baseline. No correlation between the absolute lymphocyte count and the peak engraftment was observed (fig. S2). In general, there was consistency between engraftment measured by flow cytometry and qPCR, although CART-EGFRvIII cells were detected longer by qPCR in some cases, potentially indicating persistence of genetically modified cells with loss of transgene expression, or, more likely, the higher sensitivity of qPCR compared to flow cytometry. After day 14, there was a rapid decline in the level of circulating CART-EGFRvIII cells, and all subjects had lost flow cytometry–detectable CART-EGFRvIII cells in blood by day 30 (Fig. 2A).

Although we did not observe clinical evidence of the typical cytokine release syndrome observed in patients with hematologic malignancies treated with CAR T cells, we collected serum at specified time points after CART-EGFRvIII infusion. We quantified 30 cytokines in the peripheral blood in all infused subjects. Five of the 10 subjects had 10-fold or higher elevations in IL-6, with one peak between 1 and 7 days after infusion in 4 subjects (Fig. 2B). Both subjects who received siltuximab for suspected intracranial cytokine release had significantly higher levels of IL-6 as measured in our assay after the siltuximab was infused. However, this was likely to be a false-positive measurement, because it did not correlate with clinical symptoms such as fever, or laboratory abnormalities such as elevations in C-reactive protein. It is known that cytokine-antibody pharmacodynamics are challenging to measure, and siltuximab in particular interferes with standard antibody-based measurements of IL-6 (35, 36). C-reactive protein levels were measured in subjects suspected of having cytokine release syndrome. The increased levels of IL-6 at early time points tracked with increased levels of C-reactive protein but did not correlate with the very high levels of IL-6 measured after siltuximab (Fig. 2B), confirming the likely false-positive levels of measured IL-6. Two subjects had >10-fold elevations in either IL-5 (patient 204) or IL-10 (patient 207), but no other cytokines were elevated over 10-fold from baseline in any of the subjects within the first 2 months of CART-EGFRvIII infusion (table S6).

Imaging assessments after CART-EGFRvIII infusion

All infused subjects had their disease assessed with a baseline MRI before infusion, and the first six subjects had a disease assessment MRI 4 weeks after infusion. At day 28, all but one of the subjects had stable disease as determined by post-contrast T1-weighted images. One of these subjects (207) had evidence of progression on MRI at day 28; he underwent re-resection at day 34 and was found to have progressive disease with pseudopalisading necrosis and no evidence of T cell infiltration upon neurohistopathologic evaluation (fig. S3). This subject also had one of the lowest peak levels of CART-EGFRvIII in the blood. In the other five subjects, a follow-up MRI scan at month 2 demonstrated imaging changes that were suggestive of either treatment effects or progression. For example, subject 205 had worsening contrast enhancement and T2 signal abnormality on the fluid-attenuated inversion recovery (FLAIR) images at day 28 but was considered to have stable disease by RANO criteria; she was observed closely and was clinically stable (Fig. 3A). At month 2, her imaging findings of contrast enhancement, T2 signal abnormality, and mild mass effect in the left temporal lobe progressed further (Fig. 3A). She underwent re-resection, which provided an opportunity to examine the pathological status of her disease and information regarding the trafficking and presence of CART-EGFRvIII. On pathologic evaluation, there was significant lymphocytic and macrophage infiltration and low tumor viability, which was interpreted pathologically as favoring treatment effects over true GBM progression (Fig. 3B). However, this patient died of her disease ~8 months after CART-EGFRvIII infusion (~6 months after surgery).

Another subject (209) underwent "late" surgery for a heterogeneously enhancing lesion in the left temporal lobe on day 104 after CART-EGFRvIII infusion. In the 3-month period after CART-EGFRvIII infusion, this patient's MRI imaging studies showed only incremental change that was consistently interpreted as stable disease by radiographic criteria; however, she then experienced a clinical change with increase in headaches, and therefore, the clinical team recommended surgical resection to evaluate tumor histology to guide future treatment. She underwent surgery at day 104, and postoperative MRI imaging demonstrated no residual enhancing lesion (Fig. 3C, middle panels). Follow-up MRI (T1 post-contrast images) at 7 and 12 months demonstrate a small focus of enhancement superior to the surgical cavity that remained stable over 18 months without any further therapy or interventions (Fig. 3C, bottom panels). Neuropathological examination of the surgical specimen obtained at day 104 showed infiltrative tumor with small areas of solid tumor, as well as treatment-related changes, including reactive brain parenchyma and geographic necrosis. The post-infusion tumor was less densely cellular than that of the original resection and had no pseudopalisading necrosis. A few foci of microvascular proliferation were present, and mitoses were not prominent. Collectively, these observations were felt to represent a mixed picture of treatment effects with some residual disease. This patient remains clinically stable with excellent performance status at 18 months [ECOG (Eastern Cooperative Oncology Group) grade 1]. The extent to which CART-EGFRvIII infusion contributed to this patient's clinical and radiographic stability cannot be clearly determined.

CART-EGFRvIII trafficking to the brain and effects on EGFR target expression

Seven subjects who were treated with CART-EGFRvIII had surgical resections at various intervals after the infusion. In these subjects, the post-infusion tumor was analyzed for CART-EGFRvIII cell infiltration by qPCR to assess the level of CART-EGFRvIII infiltration to brain tumor compared to peripheral blood obtained at the same time point. We found that the highest levels of CART-EGFRvIII cells in the tumor were detected at the early time points, that is, in the four subjects who had surgery within 14 days of infusion, consistent with the initial engraftment in the peripheral blood. In one subject (205), CART-EGFRvIII cells were detected in the tumor 2 months after infusion but at lower levels than in the blood; however, they were not detected at all in the subject who had the lowest level of engraftment in the blood (207) and early progression. In the subject who had surgery 3 months after CART infusion, CART-EGFRvIII was not detected in the tumor despite continued low-level detection in the peripheral blood (209) by qPCR (but not flow cytometry). CART-EGFRvIII cells were found at higher concentrations in the brain than in the peripheral blood in two subjects (216 and 217; Fig. 4A), both of whom had their tumors resected within 2 weeks of CART-EGFRvIII infusion. In these cases, CART-EGFRvIII DNA sequences were 3 or 100 times higher in brain specimens than in the peripheral blood, suggesting effective trafficking and likely expansion of CART-EGFRvIII cells in situ within active regions of GBM (Fig. 4A).

One indication of on-target effects is the decrease of antigen expression in the remaining tumor bed and tissue. In the subjects who underwent resection after CART-EGFRvIII infusion, we compared paired pre-infusion specimens to post-infusion specimens for expression of EGFRvIII (Fig. 4B) and EGFR (Fig. 4C) by the same RNA-based NGS assay used for screening. We found that expression levels of EGFRvIII declined in five of the seven infused subjects in whom post-infusion tumor was assessed ($P = 0.03$). In subject 207 [who had had poor engraftment, early progression (at month 1), and no detectable CART-EGFRvIII in the tumor], there was no effect on EGFRvIII expression. In subject 217, there were varying levels of EGFRvIII expression in multiple areas of the tumor sampled and tested, yielding a mean stable level of EGFRvIII expression after CART-EGFRvIII infusion. EGFRvIII expression decreased in the other five subjects and was undetectable in two subjects. In contrast, the level of EGFR amplification did not change in a statistically significant fashion ($P > 0.999$), suggesting that this antigen was targeted neither by CART-EGFRvIII cells nor by other tumor infiltrating lymphocytes.

In situ clonotypic T cell repertoire

On routine neuropathology evaluation, we noticed that several subjects had a robust lymphocytic infiltrate in their tumors after CART-EGFRvIII infusion, which seemed out of proportion to the level of CART-EGFRvIII genomic sequences observed (fig. S3). We sought to quantify the T cell infiltrate in subjects whose tumor was resected at different time points after infusion (day 6, day 55, and day 104 in subjects 211, 205, and 209, respectively). In these three subjects, we analyzed the T cell clonotypic repertoire in pre- and post-infusion brain tumor specimens, along with the matching infusion products, by deep sequencing the T cell receptor (TCR) Vβ chain of tumor-infiltrating T cells.

First, we found that in all three of these subjects, the number of unique TCR Vβs identified in the tumor samples increased by several thousands in post-infusion specimens, and only a small portion of these unique TCRs were shared with preexisting tumor-infiltrating specific T cells (Fig. 4D). Thus, there was a marked increase in the number and clonotypic diversity of tumor-infiltrating T cells after intravenous CART-EGFRvIII infusion.

The infusion products (derived from peripheral blood) contained many more unique clonotypes (60,000 to 80,000) than pre-infusion tumor-infiltrating lymphocytes (100 to 1000) or post-infusion tumor-infiltrating lymphocytes (2000 to 18,000). In each subject, less than 5% of the clonotypes in the infusion product was identified in the post-CART cell tumor biopsy [3226/(3226 + 61,327) in patient 205, 800/(800 + 77,794) in patient 209, and 1768/(1768 + 78,092) in patient 211]. Conversely, greater than 25% in subjects 205 and 209 and close to 10% in patient 211 of all post-infusion clonotypes in the brain biopsies were identified in the infusion product [3226/(7912 + 3226) in patient 205, 800/(800 + 2068) in patient 209, and 1768/(1768 + 16,745) in patient 211] (Fig. 4E). These data suggest that although only a small fraction of the >2.5 billion infused T cells eventually infiltrated the tumor, the clones present in the infusion product made up a relatively large fraction of the T cell repertoire infiltrating the tumor after infusion. However, we could not glean from these data whether these were the same T cell clonotypes that had been transduced with CAR.

In situ characterization of tumor-infiltrating T cells, CART-EGFRvIII cells, and the tumor microenvironment

To determine the extent to which the lymphocytic infiltrates observed in the tumors were CARTs, we developed an RNAscope in situ hybridization (RNAscope ISH) assay to detect and quantify the expression of conserved elements in the 3′ untranslated region (3′ UTR) of the CAR vector. This assay quantifies RNA molecules per cell and was validated and tested to confirm CAR expression in formalin-fixed paraffin-embedded (FFPE) tissue (fig. S4). In the patient whose tumor was resected 2 weeks after infusion (216), we detected large numbers of T cells and CART-EGFRvIII cells in situ (Fig. 5A). Compared to pre-infusion brain tumor specimens from the same patient, the post-infusion T cell infiltrate appeared to be greater, composed of more CD8 T cells, and more activated cells, based on expression of interferon-γ (IFN-γ), granzyme B, and CD25. However, in all subjects examined, the T cell infiltrate was patchy, with substantial infiltration in some areas of the tumor but not in others (Fig. 5, A and C). In all four subjects who had their tumors resected within 2 weeks of CART-EGFRvIII infusion (211, 213, 216, and 217), we detected CAR+ cells by RNAscope ISH (Fig. 5C). These T cells were composed of a mixture of CD8+ and CD8− T cells, and many had an activated phenotype.

We also evaluated the surrounding tumor microenvironment for expression of immunosuppressive molecules, including indoleamine 2,3-dioxygenase 1 (IDO1) and tryptophan 2,3-dioxygenase (TDO), programmed cell death ligand 1 (PD-L1), transforming growth factor–β (TGFβ), and IL-10 and FoxP3 as markers of regulatory T cells. All antibody stains were validated, as shown for PD-L1 in fig. S5. Compared to pre-infusion tumor specimens, post-CART–infusion tumor specimens had markedly increased expression of many immunosuppressive molecules, particularly IDO1 and FoxP3, and in some cases,

IL-10, PD-L1, and/or TGFβ (Fig. 5, B and C). The level of programmed cell death protein 1 (PD1) expression in the infiltrating lymphocytes was also assessed but did not appear to change in the post-infusion infiltrating lymphocytes compared to the pre-infusion lymphocytes (Fig. 5C). To confirm and quantify the relative percentage of FoxP3^{+} T regulatory cells, we also performed immunohistochemistry to colocalize staining of CD3 and FoxP3 (representative sample from patient 216 is shown in Fig. 6A). Because of technical incompatibility of methodologies, we were not able to colocalize CAR expression with FoxP3 staining in situ. In four of the five paired pre- and post-infusion tumor samples, we were able to detect increases in the relative proportion of FoxP3^{+} cells compared to total CD3 cells (Fig. 6B). Using similar methodology, we were also able to confirm a relative increase in proliferation of CD8 T cells in situ after CART-EGFRvIII infusion in three of the five subjects (representative sample from patient 213 shown in Fig. 6C, with quantified data for five subjects in Fig. 6D). Perhaps because of small sample size, neither the relative increase in FoxP3^{+} expression in CD3 cells nor Ki67 expression in CD8 cells met statistical significance.

Together, these findings suggest that CART-EGFRvIII trafficked from the intravenously infused product to the brain tumor, proliferated initially in situ, and exerted some direct anti-target activity, based on decreased levels of EGFRvIII expression, but this immune activation was also associated with compensatory adaptive resistance mechanisms, including up-regulation of IDO1 and PD-L1, and recruitment of IL-10–secreting, FoxP3-expressing regulatory T cells.

DISCUSSION

We conducted a first-in-human pilot study of CAR T cells directed to EGFRvIII in 10 patients with recurrent EGFRvIII[+] GBM and optimized our study to maximize the biologic information obtained from a small number of patients. Notably, our patient population consisted of heavily treated, refractory patients with multifocal, MGMT-unmethylated recurrent GBMs, a group of patients whose overall survival is extremely poor. We were able to demonstrate that manufacturing the target dose of CART-EGFRvIII cells was feasible in patients with recurrent GBM who had received multiple previous doses of temozolomide and completed a course of radiation. Even the subjects who had moderate lymphopenia had a successful manufacturing process, suggesting that the T cell dysfunction observed in GBM patients (37) does not exclude the possibility of T cell–based therapies. In terms of safety, our greatest concern during our pre-clinical development process was the possibility of cross-reactivity with wild-type EGFR; this was tested extensively in silico, in vitro, and in skin-grafted xenogeneic models (26). Reassuringly, we did not observe any evidence of cross-reactivity to wild-type EGFR in this clinical setting.

The standard of care in assessing tumor progression and responses in GBM is MRI. However, we found that imaging assessments were difficult to interpret in the setting of immunotherapy, where transient potential treatment-related changes such as inflammation could not easily be distinguished from tumor progression. In this study and in the field of brain tumor immunotherapy more generally, advanced imaging analysis is being investigated as a way to differentiate pseudo-progression and immune-related effects from true disease

progression (38, 39). We could not formally assess responses by imaging criteria in most of our patients because of their interval surgery. We observed that one patient has not required any further therapy for more than 18 months after CART infusion. We did not observe marked tumor regression by MRI in any patients. However, larger cohorts are needed to make any definitive conclusions about the potential for clinical benefit with this CART-EGFRvIII product.

The two most severe and most common toxicities of CAR T cells directed to CD19 are cytokine release syndrome and neurologic toxicity (31, 40). These two potentially but not absolutely related syndromes are related to the high tumor burden and antigen load present in patients with B cell lymphoblastic malignancies. In contrast, GBM patients are not expected to bear large tumor burdens, and thus, we did not expect or observe systemic cytokine release syndrome as manifested by fevers or hypotension. However, given the enclosed intracranial space and the potential for catastrophic localized inflammation, the possibility of localized cytokine release was considered in any subject who developed new neurologic symptoms in the first month after CART-EGFRvIII cell infusion. For this reason, two subjects received siltuximab along with corticosteroids and supportive care for new neurologic symptoms, such as seizures or worsening neurologic deficits. We chose to use siltuximab rather than tocilizumab, because although tocilizumab has an established role for the treatment of systemic cytokine release syndrome, it is not clear that tocilizumab crosses the blood-brain barrier to a sufficient degree to ameliorate neurotoxicity or brain exposure to IL-6. The mechanism of action of tocilizumab, which blocks the IL-6 receptor, transiently increases the level of IL-6 in the circulation (36), potentially exposing the brain to even higher levels of IL-6. Siltuximab binds soluble IL-6 and therefore was hypothesized to be safer for reducing CNS exposure. The only effect we observed after the administration of siltuximab was the inability to accurately measure IL-6 in the circulation afterward; fortunately, the level of C-reactive protein proved to be informative in this setting because it did not track with the increased IL-6 levels after siltuximab.

We observed that all infused subjects had detectable engraftment of CART-EGFRvIII cells in the peripheral blood, despite the relative lack of antigen in the circulation and the absence of lymphodepletion. These data suggest that CART-EGFRvIII cells had a transient growth advantage compared to the endogenous lymphocyte population, which could be related to either the ex vivo costimulation process (41) or the expression of the transgene. CAR T cells carrying the 4-1BB costimulation domain have been observed to have tonic signaling (42) and increased oxidative phosphorylation (43), which could facilitate the observed engraftment. However, CART-EGFRvIII cells engraft by 50-fold less than CD19-specific CAR T cells bearing the same 4-1BB signaling domain, lentiviral backbone, and manufacturing process, suggesting that antigen-driven expansion is more robust than CAR-mediated tonic signaling or bead (costimulation)–mediated expansion (44). Alternatively, the lower level of engraftment in the peripheral blood may in part reflect T cell homing to antigen-expressing tissues. Unlike CD19-specific CAR T cells, which encounter high numbers of antigen-bearing cells in blood, marrow, and lymphoid organs, CART-EGFRvIII cells encounter low levels of antigen only in the brain tumor. The lack of robust persistence in the peripheral blood beyond 1 month is an expected finding, and years-long persistence could be a cause for concern.

Although measuring engraftment of CART-EGFRvIII cells in the peripheral blood is a minimal requirement, we expected that efficacy of an intravenous injection would depend on the ability of CART-EGFRvIII cells to traffic to the brain, which may depend in part on the expression of VLA-4 (very late antigen–4) (45). In subjects who had a surgical resection after their CART-EGFRvIII infusion, we were able to confirm that CART-EGFRvIII cells did traffic to the tumor site. In two of these subjects, the T cells also proliferated in the brain, as measured by Ki67 staining; this is in agreement with the observed concentration gradient of CART-EGFRvIII from the tumor to the peripheral blood. We could not define the kinetics of the CART-EGFRvIII trafficking precisely, but on the basis of this study, there appears to be a defined time window of maximal and detectable trafficking of CART-EGFRvIII cells to the brain. This coincides with (or may slightly follow) the peak engraftment in the peripheral blood, at 1 to 2 weeks after infusion. Finally, we also noted the heterogeneity in T cell infiltration of brain tumors, although the exact mechanisms that drive T cell trafficking and regional infiltration are poorly understood. As larger studies of CAR T cells are performed in solid tumors, it will be interesting and important to determine what level of trafficking, proliferation, or persistence is required for the CAR T cells to exert antigen-specific activity.

We observed that most of our subjects had specific loss or decreased expression of EGFRvIII in tumors resected after CART infusion, whereas there was no change in the degree of EGFR amplification or other tumor mutations. One patient (207) who had poor expansion in blood also demonstrated no presence of CART in tumor, no antigen loss, and early disease progression. Although there are no direct ways to demonstrate the actual killing of tumor cells by CART in situ, these data, along with our preclinical data (26), support a mechanism of action of CART-EGFRvIII cells, which engraft in the peripheral blood, traffic to the brain, and exert antigen-directed cytolysis. However, on the basis of a report showing that EGFRvIII+ cells can decrease after the standard-of-care chemo-radiation therapy (46), we cannot exclude a possibility that the observed decrease of EGFRvIII+ cells was not entirely attributable to the CART therapy. In addition, EGFRvIII demonstrates complex biology and appears to fluctuate in expression over time, perhaps identifying a stem cell pool of GBM cells (47). It is intriguing to speculate that CART EGFRvIII therapy may be able to modify a subpopulation of GBM stem cells. EGFR gene amplification may be present in all cells, whereas EGFRvIII appears to be focally expressed with both spatial and temporal variations (48). These same authors showed that EGFRvIII can also be reexpressed in pools of cells that have previously lost expression, illustrating the heterogeneity of EGFRvIII expression and diverse mechanisms of regulation.

A major barrier to targeting EGFRvIII as a single antigen is the heterogeneity of its expression. In cases where several samples of brain tumor were collected and analyzed separately, we noted wide regional variation of EGFRvIII expression by our highly quantitative assay. We also noted significant tumor heterogeneity for other mutations in EGFR. In some cases, after CART infusion, there was loss of other missense mutations in EGFR, with retention of other mutations such as PIK3CA and EGFR amplification. This suggests that in at least some cases, EGFRvIII may not be an early or initiating mutation. One of the main questions that this study invokes is whether successful targeting of EGFRvIII will translate into a durable clinical benefit or whether antigen escape will occur so rapidly and frequently that there is minimal clinical impact from targeting EGFRvIII

alone. EGFRvIII antigen escape has been observed in other vaccination-based studies (16), but the frequency and kinetics of this escape could vary.

A major observation from this study is the effect of CART-EGFRvIII cells on the tumor microenvironment. We found that within the first 2 weeks of CART-EGFRvIII infusion, there was efficient trafficking of CART cells to the brain tumor, but there was also a much greater influx of nontransduced, polyclonal T cells, suggesting a secondary response by non–CAR-expressing T cells. At first blush, the possibility of epitope spreading induced by CART-EGFRvIII and possibly resulting in recognition of native or mutated tumor antigens was encouraging, given that the presence of lymphocytes within malignant gliomas can be a positive prognostic indicator of survival (49, 50). However, in situ phenotypic analysis of the post-infusion T cell infiltrate indicated that many of these cells appeared to be immunosuppressive regulatory T cells, based on their expression of CD4, CD25, and FoxP3. In addition, compared to pre-CART tumor specimens, there was consistent up-regulation of expression of other immunosuppressive molecules such as IDO1, PD-L1, and IL-10 after CART-EGFRvIII infusion. This observation suggests that CART-EGFRvIII activation induced a compensatory multifactorial immunosuppressive response in situ, perhaps driven by an initial production of IFN-γ. This also suggests the possibility of synergy between CAR T cells and inhibition of IDO1 with small-molecule drugs and/or the PD1/PD-L1 axis with checkpoint blocking antibodies.

In conclusion, our study demonstrated that manufacturing of CART-EGFRvIII cells from patients with recurrent GBM is feasible and that there was no cross-reactivity of wild-type EGFR with our construct. Any clinical benefit could not be definitively determined from this small study, but we observed that CART-EGFRvIII cells infused intravenously did traffic to the brain tumor and exert antigen-directed activity. The major barriers to clinical efficacy of this therapy are the heterogeneity of EGFRvIII expression and the inhibitory tumor microenvironment, which becomes even more immunosuppressive after CART cells. Although the former will require targeting additional antigens, the latter may be overcome with existing drugs that target immunosuppressive molecules.

MATERIALS AND METHODS

Study design

This clinical trial was a phase 1 open-label study where the primary objectives were safety and feasibility. The study was designed to screen an unlimited number of tumor samples and infuse up to 12 patients. Safety was determined according to National Cancer Institute's Common Terminology Criteria for Adverse Events version 4.0. Manufacturing feasibility was defined as the frequency of the inability to prepare a dose of at least 1×10^7 CART-EGFRvIII. Clinical feasibility was defined as the ability to infuse subjects who had their CART-EGFRvIII product manufactured. No dose escalation was planned, but dose de-escalation was planned if there were >33% of the subjects experiencing a dose-limiting toxicity, defined as a grade 3 or higher toxicity that was unexpected and attributable to CART-EGFRvIII. The study was approved by the Recombinant DNA Advisory Committee, FDA, Abramson Cancer Center Clinical Trials Scientific Review Committee, and the Penn Institutional Biosafety Committee and Institutional Review Board. The clinical trial

(NCT02209376) was conducted as outlined in Fig. 1A. Patients with newly diagnosed or recurrent GBM were eligible for screening for EGFRvIII expression in their resected tumor specimen. Patients with confirmed EGFRvIII expression were eligible for leukapheresis and having their CART-EGFRvIII cells manufactured on step 1 of this study. Peripheral blood T cells were stimulated and transduced with a lentiviral vector encoding the CAR: humanized anti-EGFRvIII single-chain variable fragment fused to the hinge and transmembrane domain of CD8 and the human 4-1BB and CD3ζ intracellular signaling domains. CART-EGFRvIII cells were manufactured at the Cell and Vaccine Production Facility at the University of Pennsylvania, which operates under good manufacturing practices. CART-EGFRvIII cells were formulated and cryopreserved until the patient was eligible and consented for treatment. CART-EGFRvIII cells were administered by a single intravenous infusion.

EGFRvIII NGS assay

Biopsy specimens were sent as rolls from FFPE when the estimated tumor percentages were greater than 50% or as slides, which were macrodissected when the tumor percentage was less than 50%. Total nucleic acids were extracted from the tissue using Agencourt FormaPure (Beckman Coulter). Complementary DNA was synthesized from material equivalent of 200 ng of RNA based on the RNA Qubit (Thermo Fisher Scientific) reading. PCR primers were designed to capture wild-type EGFR spanning exons 1 and 2, EGFRvIII spanning exons 1 to 8, and three housekeeping genes (HPRT, SDHA, and RPL13A). The assay also includes three primer sets with increasing target sizes built in the assay; this allows for assessment of the RNA degradation level of the sample in a single assay [exons 9 to 9, 93 base pairs (bp); exons 9 to 10, 141 bp; exons 9 to 12, 251 bp]. The NGS library preparation is a two-step PCR method: The first step is a multiplex PCR followed by second PCR to add Illumina sequencing index and adaptors. Subsequently, the sequencing library is quantitated on TapeStation (Agilent) and then sequenced on MiSeq (Illumina). A custom bioinformatics pipeline was developed to process the data. EGFRvIII ratio is calculated by the following formula built in the bioinformatics pipeline: EGFRvIII ratio = (EGFRvIII reads)/(EGFRvIII reads + WT EGFR reads).

Measurement of transgene persistence in vivo

Research sample processing, freezing, and laboratory analyses were performed in the Translational and Correlative Studies Laboratory at the University of Pennsylvania, using established standard operating procedures (SOPs) and/or protocols for sample receipt, processing, freezing, and analysis.

CART-EGFRvIII cells were quantified from peripheral blood samples obtained at protocol-specified time points. Samples (peripheral blood) were collected in lavender top (K2EDTA) or red top (no additive) Vacutainer tubes (Becton Dickinson). Lavender top tubes were delivered to the laboratory within 2 hours of the sample draw. Samples were processed within 16 hours of drawing according to the established SOP. PBMCs were purified, processed, and stored in the vapor phase of liquid nitrogen. Red top tubes were processed within 2 hours of the draw including coagulation time, and serum was isolated by centrifugation, aliquoted, and stored at −80°C.

Cells were evaluated by flow cytometry directly after Ficoll-Paque processing. Immunophenotyping of PBMC was performed using about 2×10^5 to 5×10^5 total cells per condition depending on cell yield in samples. FMO (fluorescence minus one) secondary only controls were used for CAR-EGFRvIII evaluation. Reagents and protocols used for flow cytometry are described in the Supplementary Materials.

Genomic DNA was isolated directly from whole blood, and qPCR analysis was performed using ABI TaqMan technology and a validated assay to detect the integrated CAR transgene sequence as described (51) using triplicates of 200 ng of genomic DNA per time point for peripheral blood and marrow samples. To determine copy number per unit DNA, an eight-point standard curve was generated consisting of 5 to 10^6 copies of lentivirus plasmid spiked into 100 ng of nontransduced control genomic DNA. The number of copies of plasmid present in the standard curve was verified using digital qPCR with the same primer/probe set and performed on a QuantStudio 3D digital PCR instrument (Life Technologies). Each datapoint (sample and standard curve) was evaluated in triplicate with a positive C_t value in three of three replicates with percent coefficient of variation of less than 0.95% for all quantifiable values. To control for the quality of interrogated DNA, we performed a parallel amplification reaction using 20 ng of genomic DNA and a primer/probe combination specific for a non-transcribed genomic sequence upstream of the CDKN1A (p21) gene as described (28). These amplification reactions generated a correction factor to adjust for calculated versus actual DNA input. Copies of trans-gene per microgram of DNA were calculated according to the formula: copies per microgram of genomic DNA = (copies calculated from CART-EGFRvIII standard curve) × correction factor/(amount DNA evaluated in nanograms) × 1000 ng.

NGS of TCRβ gene rearrangements

Genomic DNA was extracted from tumor biopsies before and after CART-EGFRvIII therapy and from the infusion product, and the third complementarity-determining regions of the TCRβ locus were amplified and deep-sequenced (Adaptive Technologies). Data analysis was performed using ImmunoSEQ or exported and examined using Excel or Prism. For bivariate analysis of the pre- versus post-CART and infusion product versus post-CART cell samples, log scatter data were exported to Excel. Zero values were converted to 0.0001 using Excel, and the resultant data were imported into Prism.

Immunohistochemistry and RNAscope ISH

For immunohistochemistry, FFPE tissues were used. As outlined below, molecular localization studies were conducted using a Ventana Discovery Ultra autostainer. In brief, tissues were sectioned at 5 μm, barcoded, and then placed in the autostainer for paraffin extraction and rehydration [EZ Prep (Ventana #950-100)]. The antibodies and final concentrations are described in table S2. We used the SP263 Ventana PD-L1 immunohistochemistry assay, an approved companion diagnostic for nivolumab. Antigen retrieval [CC1 (Ventana #950-124)], primary antibody dilution, incubation temperature and duration, detection technique, and 3,3′-diaminobenzidine chromogen [ChromoMap DAB Kit (Ventana #760-159)] were optimized on nonstudy archived tissue and included evaluation of isotype-matched irrelevant antibody controls and known negative and positive

tissues. Slides were counterstained [hematoxylin (Ventana #760-2021)] and coverslipped [Micromount (Leica Biosystems #3801731)]. For photomicrographs, slides were scanned at ×20 magnification using an Aperio slide AT2 scanner (Leica Biosystems). Individual images were captured with an Olympus BX46 microscope coupled to an Olympus DP72 digital camera and DP2-BSW imaging software or Nuance spectral imaging system (PerkinElmer). Quantitative image analysis was performed using Halo software cytonuclear and multiplex modules IHC (Indica Labs).

ISH was performed using Advanced Cell Diagnostics (ACDBio)/Ventana Medical Systems (Roche Group) probes and reagents. The CAR-3′UTR (catalog #438086) and IFN-γ (catalog #310501) probes (table S5) were designed by ACD using the CAR construct accession no. KJ698853.1 (covering the region of nucleotides 64 to 854) and the IFN-γ accession no. NM_000619 (covering the region of nucleotides 80 to 1152), respectively. Tumor processing and the reagents and protocols used for ISH are described in the Supplementary Materials.

Statistics

Because of the small sample size of patients, the majority of this study is descriptive. In evaluating EGFRvIII expression and EGFR amplification, the Wilcoxon matched-pairs signed-rank test was used to evaluate significance in before and after samples from the same patient. Spearman correlations were used to determine significance between two variables.

Supplementary Material

Refer to Web version on PubMed Central for supplementary material.

Acknowledgments

REFERENCES AND NOTES

1. Stupp R, Mason WP, van den Bent MJ, Weller M, Fisher B, Taphoorn MJB, Belanger K, Brandes AA, Marosi C, Bogdahn U, Curschmann J, Janzer RC, Ludwin SK, Gorlia T, Allgeier A, Lacombe D, Cairncross JG, Eisenhauer E, Mirimanoff RO. European Organisation for Research and Treatment of Cancer Brain Tumor and Radiotherapy Groups; National Cancer Institute of Canada Clinical Trials Group. Radiotherapy plus concomitant and adjuvant temozolomide for glioblastoma. N Engl J Med. 2005; 352:987–996. [PubMed: 15758009]

2. Chi AS, Norden AD, Wen PY. Antiangiogenic strategies for treatment of malignant gliomas. Neurotherapeutics. 2009; 6:513–526. [PubMed: 19560741]

3. Verhoeff JJC, van Tellingen O, Claes A, Stalpers LJA, van Linde ME, Richel DJ, Leenders WPJ, van Furth WR. Concerns about anti-angiogenic treatment in patients with glioblastoma multiforme. BMC Cancer. 2009; 9:444. [PubMed: 20015387]

4. Sathornsumetee S, Reardon DA. Targeting multiple kinases in glioblastoma multiforme. Expert Opin Investig Drugs. 2009; 18:277–292.

5. Stupp R, Taillibert S, Kanner AA, Kesari S, Steinberg DM, Toms SA, Taylor LP, Lieberman F, Silvani A, Fink KL, Barnett GH, Zhu JJ, Henson JW, Engelhard HH, Chen TC, Tran DD, Sroubek J, Tran ND, Hottinger AF, Landolfi J, Desai R, Caroli M, Kew Y, Honnorat J, Idbaih A, Kirson ED, Weinberg U, Palti Y, Hegi ME, Ram Z. Maintenance therapy with tumor-treating fields plus temozolomide vs temozolomide alone for glioblastoma: A randomized clinical trial. JAMA. 2015; 314:2535–2543. [PubMed: 26670971]

6. Patil CG, Yi A, Elramsisy A, Hu J, Mukherjee D, Irvin DK, Yu JS, Bannykh SI, Black KL, Nuño M. Prognosis of patients with multifocal glioblastoma: A case-control study. J Neurosurg. 2012; 117:705–711. [PubMed: 22920963]

7. Rivera AL, Pelloski CE, Gilbert MR, Colman H, De La Cruz C, Sulman EP, Bekele BN, Aldape KD. MGMT promoter methylation is predictive of response to radiotherapy and prognostic in the absence of adjuvant alkylating chemotherapy for glioblastoma. Neuro Oncol. 2010; 12:116–121. [PubMed: 20150378]

8. Esteller M, Garcia-Foncillas J, Andion E, Goodman SN, Hidalgo OF, Vanaclocha V, Baylin SB, Herman JG. Inactivation of the DNA-repair gene *MGMT* and the clinical response of gliomas to alkylating agents. N Engl J Med. 2000; 343:1350–1354. [PubMed: 11070098]

9. Li G, Wong AJ. EGF receptor variant III as a target antigen for tumor immunotherapy. Expert Rev Vaccines. 2008; 7:977–985. [PubMed: 18767947]

10. Padfield E, Ellis HP, Kurian KM. Current therapeutic advances targeting EGFR and EGFRvIII in glioblastoma. Front Oncol. 2015; 5:5. [PubMed: 25688333]

11. Heimberger AB, Suki D, Yang D, Shi W, Aldape K. The natural history of EGFR and EGFRvIII in glioblastoma patients. J Transl Med. 2005; 3:38. [PubMed: 16236164]

12. Heimberger AB, Hlatky R, Suki D, Yang D, Weinberg J, Gilbert M, Sawaya R, Aldape K. Prognostic effect of epidermal growth factor receptor and EGFRvIII in glioblastoma multiforme patients. Clin Cancer Res. 2005; 11:1462–1466. [PubMed: 15746047]

13. Tykocinski ES, Grant RA, Kapoor GS, Krejza J, Bohman LE, Gocke TA, Chawla S, Halpern CH, Lopinto J, Melhem ER, O'Rourke DM. Use of magnetic perfusion-weighted imaging to determine epidermal growth factor receptor variant III expression in glioblastoma. Neuro Oncol. 2012; 14:613–623. [PubMed: 22492960]

14. Thorne AH, Zanca C, Furnari F. Epidermal growth factor receptor targeting and challenges in glioblastoma. Neuro Oncol. 2016; 18:914–918. [PubMed: 26755074]

15. Schuster J, Lai RK, Recht LD, Reardon DA, Paleologos NA, Groves MD, Mrugala MM, Jensen R, Baehring JM, Sloan A, Archer GE, Bigner DD, Cruickshank S, Green JA, Keler T, Davis TA, Heimberger AB, Sampson JH. A phase II, multicenter trial of rindopepimut (CDX-110) in newly diagnosed glioblastoma: The ACT III study. Neuro Oncol. 2015; 17:854–861. [PubMed: 25586468]

16. Sampson JH, Heimberger AB, Archer GE, Aldape KD, Friedman AH, Friedman HS, Gilbert MR, Herndon JE II, McLendon RE, Mitchell DA, Reardon DA, Sawaya R, Schmittling RJ, Shi W, Vredenburgh JJ, Bigner DD. Immunologic escape after prolonged progression-free survival with epidermal growth factor receptor variant III peptide vaccination in patients with newly diagnosed glioblastoma. J Clin Oncol. 2010; 28:4722–4729. [PubMed: 20921459]

17. Maude SL, Frey N, Shaw PA, Aplenc R, Barrett DM, Bunin NJ, Chew A, Gonzalez VE, Zheng Z, Lacey SF, Mahnke YD, Melenhorst JJ, Rheingold SR, Shen A, Teachey DT, Levine BL, June CH, Porter DL, Grupp SA. Chimeric antigen receptor T cells for sustained remissions in leukemia. N Engl J Med. 2014; 371:1507–1517. [PubMed: 25317870]

18. Turtle CJ, Hanafi LA, Berger C, Gooley TA, Cherian S, Hudecek M, Sommermeyer D, Melville K, Pender B, Budiarto TM, Robinson E, Steevens NN, Chaney C, Soma L, Chen X, Yeung C, Wood B, Li D, Cao J, Heimfeld S, Jensen MC, Riddell SR, Maloney DG. CD19 CAR-T cells of defined CD4$^+$:CD8$^+$ composition in adult B cell ALL patients. J Clin Invest. 2016; 126:2123–2138. [PubMed: 27111235]

19. Porter DL, Hwang WT, Frey NV, Lacey SF, Shaw PA, Loren AW, Bagg A, Marcucci KT, Shen A, Gonzalez V, Ambrose D, Grupp SA, Chew A, Zheng Z, Milone MC, Levine BL, Melenhorst JJ,

June CH. Chimeric antigen receptor T cells persist and induce sustained remissions in relapsed refractory chronic lymphocytic leukemia. Sci Transl Med. 2015; 7:303ra139.

20. Kochenderfer JN, Dudley ME, Kassim SH, Somerville RPT, Carpenter RO, Stetler-Stevenson M, Yang JC, Phan GQ, Hughes MS, Sherry RM, Raffeld M, Feldman S, Lu L, Li YF, Ngo LT, Goy A, Feldman T, Spaner DE, Wang ML, Chen CC, Kranick SM, Nath A, Nathan DA, Morton KE, Toomey MA, Rosenberg SA. Chemotherapy-refractory diffuse large B-cell lymphoma and indolent B-cell malignancies can be effectively treated with autologous T cells expressing an anti-CD19 chimeric antigen receptor. J Clin Oncol. 2015; 33:540–549. [PubMed: 25154820]

21. Kershaw MH, Westwood JA, Parker LL, Wang G, Eshhar Z, Mavroukakis SA, White DE, Wunderlich JR, Canevari S, Rogers-Freezer L, Chen CC, Yang JC, Rosenberg SA, Hwu P. A phase I study on adoptive immunotherapy using gene-modified T cells for ovarian cancer. Clin Cancer Res. 2006; 12(Pt 1):6106–6115. [PubMed: 17062687]

22. Beatty GL, Haas AR, Maus MV, Torigian DA, Soulen MC, Plesa G, Chew A, Zhao Y, Levine BL, Albelda SM, Kalos M, June CH. Mesothelin-specific chimeric antigen receptor mRNA-engineered T cells induce anti-tumor activity in solid malignancies. Cancer Immunol Res. 2014; 2:112–120. [PubMed: 24579088]

23. Ahmed N, Brawley VS, Hegde M, Robertson C, Ghazi A, Gerken C, Liu E, Dakhova O, Ashoori A, Corder A, Gray T, Wu MF, Liu H, Hicks J, Rainusso N, Dotti G, Mei Z, Grilley B, Gee A, Rooney CM, Brenner MK, Heslop HE, Wels WS, Wang LL, Anderson P, Gottschalk S. Human epidermal growth factor receptor 2 (HER2)-specific chimeric antigen receptor-modified T cells for the immunotherapy of HER2-positive sarcoma. J Clin Oncol. 2015; 33:1688–1696. [PubMed: 25800760]

24. Brown CE, Alizadeh D, Starr R, Weng L, Wagner JR, Naranjo A, Ostberg JR, Blanchard MS, Kilpatrick J, Simpson J, Kurien A, Priceman SJ, Wang X, Harshbarger TL, D'Apuzzo M, Ressler JA, Jensen MC, Barish ME, Chen M, Portnow J, Forman SJ, Badie B. Regression of glioblastoma after chimeric antigen receptor T-cell therapy. N Engl J Med. 2016; 375:2561–2569. [PubMed: 28029927]

25. Ohno M, Ohkuri T, Kosaka A, Tanahashi K, June CH, Natsume A, Okada H. Expression of miR-17-92 enhances anti-tumor activity of T-cells transduced with the anti-EGFRvIII chimeric antigen receptor in mice bearing human GBM xenografts. J Immunother Cancer. 2013; 1:21. [PubMed: 24829757]

26. Johnson LA, Scholler J, Ohkuri T, Kosaka A, Patel PR, McGettigan SE, Nace AK, Dentchev T, Thekkat P, Loew A, Boesteanu AC, Cogdill AP, Chen T, Fraietta JA, Kloss CC, Posey AD Jr, Engels B, Singh R, Ezell T, Idamakanti N, Ramones MH, Li N, Zhou L, Plesa G, Seykora JT, Okada H, June CH, Brogdon JL, Maus MV. Rational development and characterization of humanized anti–EGFR variant III chimeric antigen receptor T cells for glioblastoma. Sci Transl Med. 2015; 7:275ra22.

27. Hegi ME, Liu L, Herman JG, Stupp R, Wick W, Weller M, Mehta MP, Gilbert MR. Correlation of O^6-methylguanine methyltransferase (MGMT) promoter methylation with clinical outcomes in glioblastoma and clinical strategies to modulate MGMT activity. J Clin Oncol. 2008; 26:4189–4199. [PubMed: 18757334]

28. Kalos M, Levine BL, Porter DL, Katz S, Grupp SA, Bagg A, June CH. T cells with chimeric antigen receptors have potent antitumor effects and can establish memory in patients with advanced leukemia. Sci Transl Med. 2011; 3:95ra73.

29. Porter DL, Levine BL, Kalos M, Bagg A, June CH. Chimeric antigen receptor-modified T cells in chronic lymphoid leukemia. N Engl J Med. 2011; 365:725–733. [PubMed: 21830940]

30. Levine BL, Miskin J, Wonnacott K, Keir C. Global manufacturing of CAR T cell therapy. Mol Ther Methods Clin Dev. 2017; 4:92–101. [PubMed: 28344995]

31. Maude SL, Barrett D, Teachey DT, Grupp SA. Managing cytokine release syndrome associated with novel T cell-engaging therapies. Cancer J. 2014; 20:119–122. [PubMed: 24667956]

32. Teachey DT, Rheingold SR, Maude SL, Zugmaier G, Barrett DM, Seif AE, Nichols KE, Suppa EK, Kalos M, Berg RA, Fitzgerald JC, Aplenc R, Gore L, Grupp SA. Cytokine release syndrome after blinatumomab treatment related to abnormal macrophage activation and ameliorated with cytokine directed therapy. Blood. 2013; 121:5154–5157. [PubMed: 23678006]

33. Teachey DT, Lacey SF, Shaw PA, Melenhorst JJ, Maude SL, Frey N, Pequignot E, Gonzalez VE, Chen F, Finklestein J, Barrett DM, Weiss SL, Fitzgerald JC, Berg RA, Aplenc R, Callahan C, Rheingold SR, Zheng Z, Rose-John S, White JC, Nazimuddin F, Wertheim G, Levine BL, June CH, Porter DL, Grupp SA. Identification of predictive biomarkers for cytokine release syndrome after chimeric antigen receptor T-cell therapy for acute lymphoblastic leukemia. Cancer Discov. 2016; 6:664–679. [PubMed: 27076371]

34. Paulos CM, Suhoski MM, Plesa G, Jiang T, Basu S, Golovina TN, Jiang S, Aqui NA, Powell DJ Jr, Levine BL, Carroll RG, Riley JL, June CH. Adoptive immunotherapy: Good habits instilled at youth have long-term benefits. Immunol Res. 2008; 42:182–196. [PubMed: 18949448]

35. Wang W, Wang X, Doddareddy R, Fink D, McIntosh T, Davis HM, Zhou H. Mechanistic pharmacokinetic/target engagement/pharmacodynamic (PK/TE/PD) modeling in deciphering interplay between a monoclonal antibody and its soluble target in cynomolgus monkeys. AAPS J. 2014; 16:129–139. [PubMed: 24287601]

36. Chen F, Teachey DT, Pequignot E, Frey N, Porter D, Maude SL, Grupp SA, June CH, Melenhorst JJ, Lacey SF. Measuring IL-6 and sIL-6R in serum from patients treated with tocilizumab and/or siltuximab following CAR T cell therapy. J Immunol Methods. 2016; 434:1–8. [PubMed: 27049586]

37. Grossman SA, Ye X, Lesser G, Sloan A, Carraway H, Desideri S, Piantadosi S. Consortium NABTTCNS. Immunosuppression in patients with high-grade gliomas treated with radiation and temozolomide. Clin Cancer Res. 2011; 17:5473–5480. [PubMed: 21737504]

38. Okada H, Weller M, Huang R, Finocchiaro G, Gilbert MR, Wick W, Ellingson BM, Hashimoto N, Pollack IF, Brandes AA, Franceschi E, Herold-Mende C, Nayak L, Panigrahy A, Pope WB, Prins R, Sampson JH, Wen PY, Reardon DA. Immunotherapy response assessment in neuro-oncology: A report of the RANO working group. Lancet Oncol. 2015; 16:e534–e542. [PubMed: 26545842]

39. Reardon DA, Okada H. Re-defining response and treatment effects for neuro-oncology immunotherapy clinical trials. J Neurooncol. 2015; 123:339–346. [PubMed: 25707876]

40. Lee DW, Gardner R, Porter DL, Louis CU, Ahmed N, Jensen M, Grupp SA, Mackall CL. Current concepts in the diagnosis and management of cytokine release syndrome. Blood. 2014; 124:188–195. [PubMed: 24876563]

41. Laport GG, Levine BL, Stadtmauer EA, Schuster SJ, Luger SM, Grupp S, Bunin N, Strobl FJ, Cotte J, Zheng Z, Gregson B, Rivers P, Vonderheide RH, Liebowitz DN, Porter DL, June CH. Adoptive transfer of costimulated T cells induces lymphocytosis in patients with relapsed/refractory non-Hodgkin lymphoma following CD34+-selected hematopoietic cell transplantation. Blood. 2003; 102:2004–2013. [PubMed: 12763934]

42. Long AH, Haso WM, Shern JF, Wanhainen KM, Murgai M, Ingaramo M, Smith JP, Walker AJ, Kohler ME, Venkateshwara VR, Kaplan RN, Patterson GH, Fry TJ, Orentas RJ, Mackall CL. 4-1BB costimulation ameliorates T cell exhaustion induced by tonic signaling of chimeric antigen receptors. Nat Med. 2015; 21:581–590. [PubMed: 25939063]

43. Kawalekar OU, O'Connor RS, Fraietta JA, Guo L, McGettigan SE, Posey AD Jr, Patel PR, Guedan S, Scholler J, Keith B, Snyder NW, Blair IA, Milone MC, June CH. Distinct signaling of coreceptors regulates specific metabolism pathways and impacts memory development in CAR T cells. Immunity. 2016; 44:380–390. [PubMed: 26885860]

44. Rapoport AP, Stadtmauer EA, Aqui N, Vogl D, Chew A, Fang HB, Janofsky S, Yager K, Veloso E, Zheng Z, Milliron T, Westphal S, Cotte J, Huynh H, Cannon A, Yanovich S, Akpek G, Tan M, Virts K, Ruehle K, Harris C, Philip S, Vonderheide RH, Levine BL, June CH. Rapid immune recovery and graft-versus-host disease–like engraftment syndrome following adoptive transfer of costimulated autologous T cells. Clin Cancer Res. 2009; 15:4499–4507. [PubMed: 19509133]

45. Sasaki K, Zhu X, Vasquez C, Nishimura F, Dusak JE, Huang J, Fujita M, Wesa A, Potter DM, Walker PR, Storkus WJ, Okada H. Preferential expression of very late antigen-4 on type 1 CTL cells plays a critical role in trafficking into central nervous system tumors. Cancer Res. 2007; 67:6451–6458. [PubMed: 17616706]

46. van den Bent MJ, Gao Y, Kerkhof M, Kros JM, Gorlia T, van Zwieten K, Prince J, van Duinen S, Sillevis Smitt PA, Taphoorn M, French PJ. Changes in the EGFR amplification and EGFRvIII expression between paired primary and recurrent glioblastomas. Neuro Oncol. 2015; 17:935–941. [PubMed: 25691693]

47. Del Vecchio CA, Jensen KC, Nitta RT, Shain AH, Giacomini CP, Wong AJ. Epidermal growth factor receptor variant III contributes to cancer stem cell phenotypes in invasive breast carcinoma. Cancer Res. 2012; 72:2657–2671. [PubMed: 22419663]

48. Del Vecchio CA, Giacomini CP, Vogel H, Jensen KC, Florio T, Merlo A, Pollack JR, Wong AJ. EGFRvIII gene rearrangement is an early event in glioblastoma tumorigenesis and expression defines a hierarchy modulated by epigenetic mechanisms. Oncogene. 2013; 32:2670–2681. [PubMed: 22797070]

49. Palma L, Di Lorenzo N, Guidetti B. Lymphocytic infiltrates in primary glioblastomas and recidivous gliomas. Incidence, fate, and relevance to prognosis in 228 operated cases. J Neurosurg. 1978; 49:854–861. [PubMed: 731302]

50. Brooks WH, Markesbery WR, Gupta GD, Roszman TL. Relationship of lymphocyte invasion and survival of brain tumor patients. Ann Neurol. 1978; 4:219–224. [PubMed: 718133]

51. Janetzki S, Britten CM, Kalos M, Levitsky HI, Maecker HT, Melief CJM, Old LJ, Romero P, Hoos A, Davis MM. "MIATA"—Minimal information about T cell assays. Immunity. 2009; 31:527–528. [PubMed: 19833080]
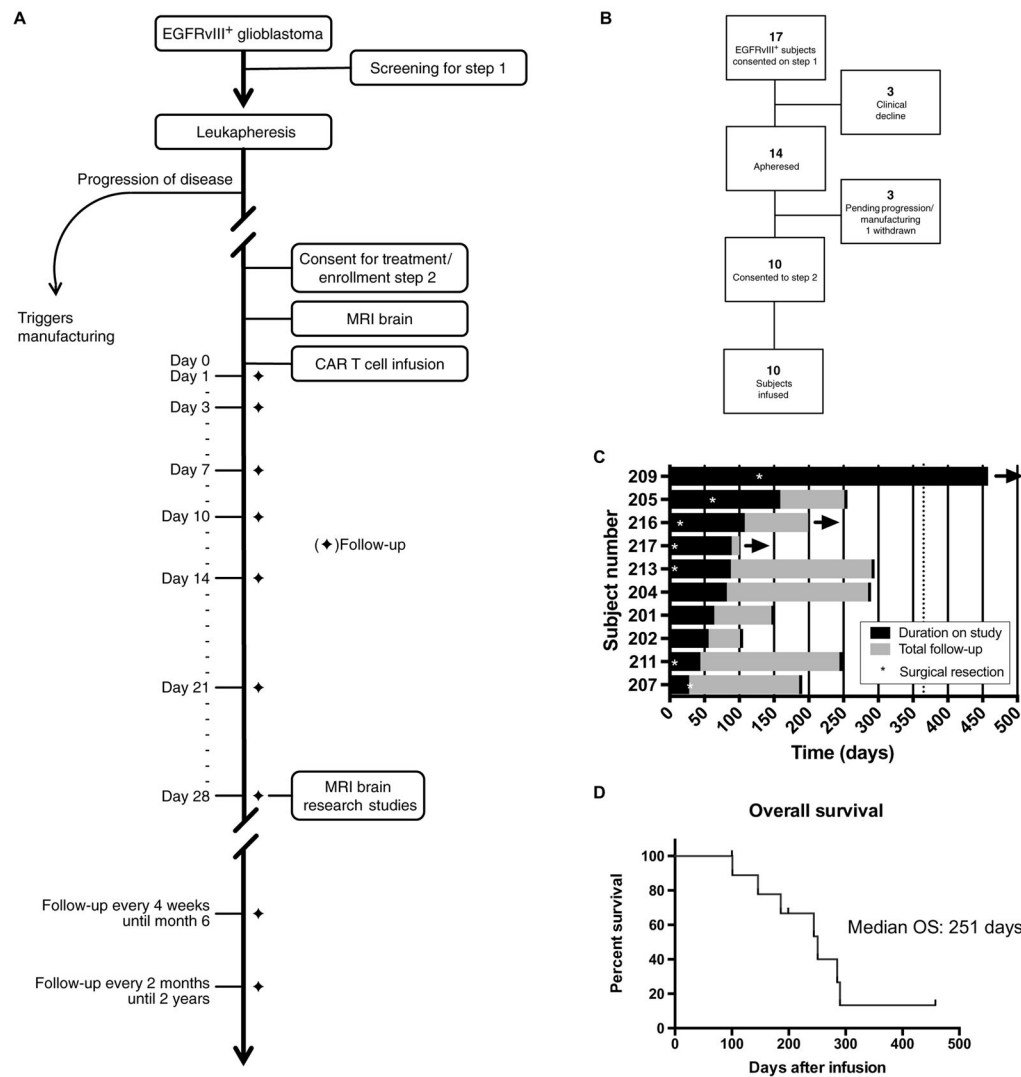
Fig. 1. Protocol design, consort diagram, and clinical outcomes in subjects infused with CART-EGFRvIII

(**A**) Protocol schema for EGFRvIII testing, leukapheresis, and manufacturing, treatment with CAR T cells directed to EGFRvIII, and follow-up. (**B**) Consort diagram indicating the number of subjects screened and enrolled on the study. (**C**) Swimmer's plot describing time on study for each subject (black), duration of follow-up off study (that is, survival beyond progression or initiation of other therapy) (gray), and present status. Arrows indicate ongoing survival. Asterisks indicate surgical intervention. Dashed vertical line indicates 1-year time point. (**D**) OS plotted as Kaplan-Meier estimate for all subjects. *X* axis is shown in days. Tick marks indicate each censored subject (that is, subjects who are alive at the data cutoff point).
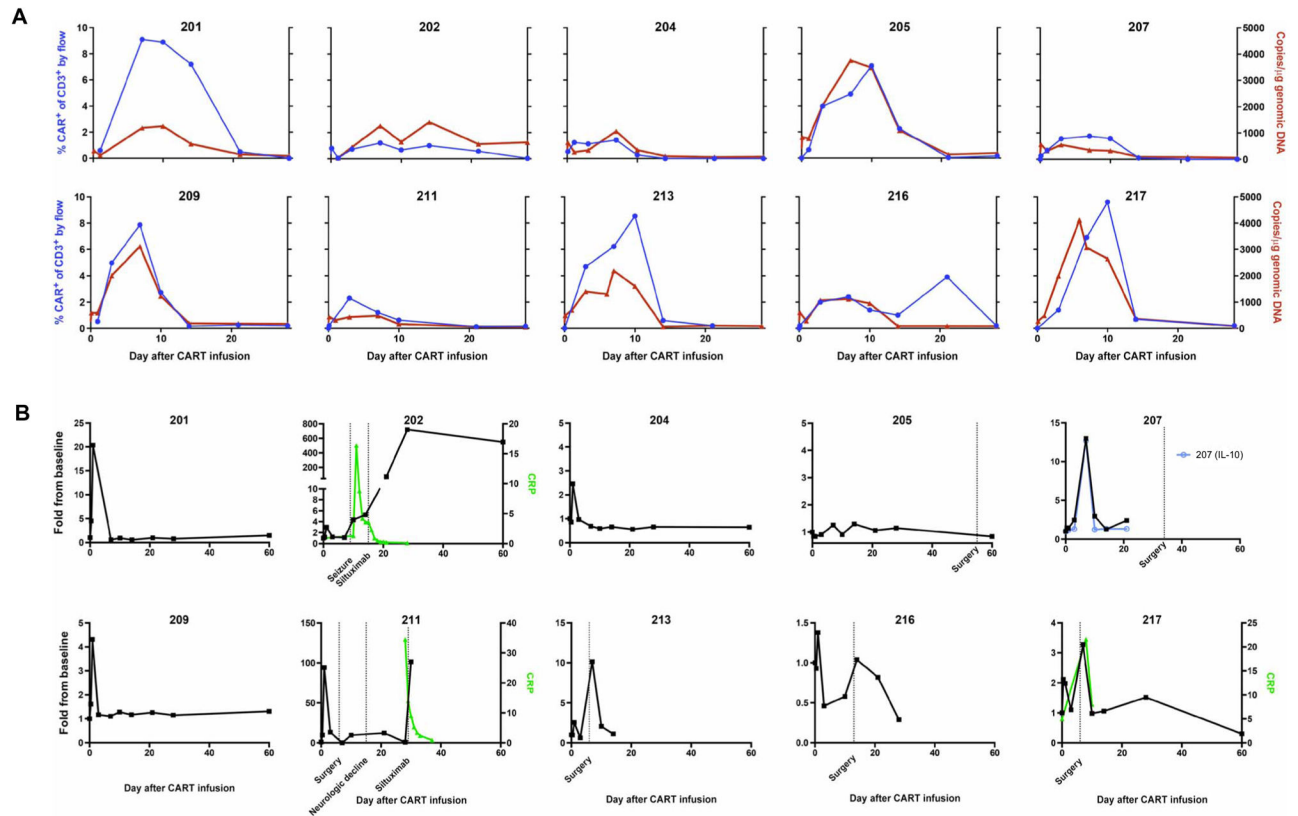
Fig. 2. Engraftment of CART-EGFRvIII and cytokine modulation in the peripheral blood
(**A**) CART-EGFRvIII engraftment and persistence in the peripheral blood by flow cytometry detecting the CAR on $CD3^+$ T cells (left y axis, blue curve) and by qPCR detecting CAR sequences (right y axis, red curve) in PBMC genomic DNA. Pharmacokinetics over the first 30 days for each subject are shown. (**B**) Fold change in IL-6 levels in the peripheral blood of each subject over time (black squares, plotted on the left y axis). Baseline IL-6 levels for subjects 201, 202, 204, 205, 207, 209, 211, 213, 216, and 217 were 2.57, 7.5, 8.58, 4.90, 1.78, 4.40, 0.35, 3.11, 8.89, and 33.85 pg/ml, respectively. Baseline level of IL-10 in subject 207 was 2.03 pg/ml. Data for all other cytokines are shown in table S6. C-reactive protein (CRP) levels are plotted in the subjects in whom it was measured over time (green triangles, right y axis). Significant clinical events such as seizures, surgery, or administration of siltuximab are noted on the x axis.
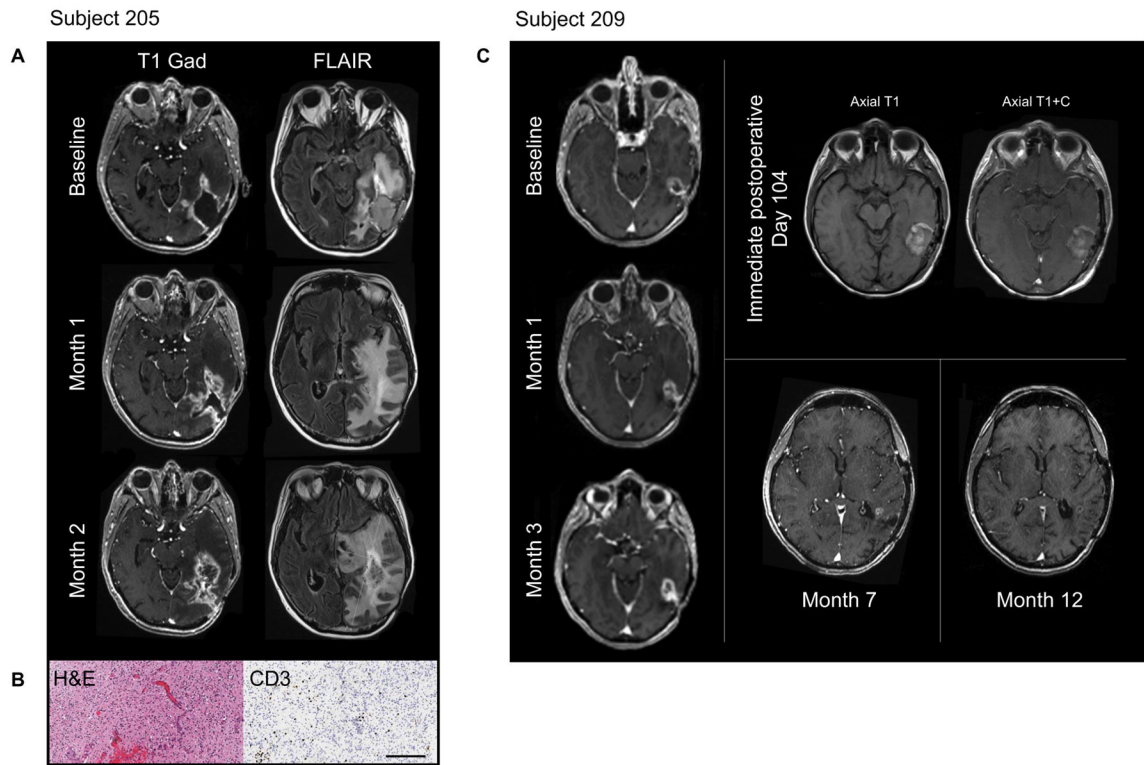
Fig. 3. Effects of CART-EGFRvIII on radiological and/or pathological assessments in two subjects

(**A**) MRI performed before and after administration of gadolinium (gad) in subject 205. T1 post-contrast and FLAIR images are shown for the indicated time points. (**B**) Histological analysis of surgical specimens obtained from subject 205, 2 months after CART-EGFRvIII infusion. Hematoxylin and eosin (H&E)–stained sections and immunohistochemistry for CD3 to demonstrate T cells are shown. Scale bar, 200 μm. (**C**) MRI (T1 post-contrast images) shown at the indicated time points for subject 209. This subject underwent surgical resection of one portion of the tumor after the 3-month scan.
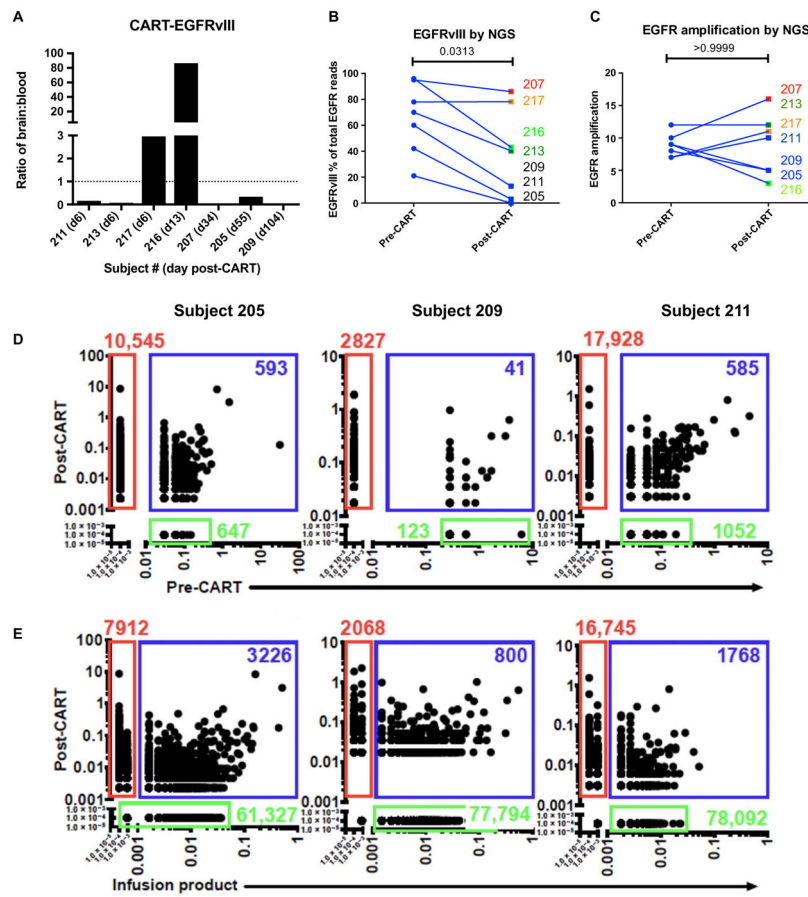
Fig. 4. T cell trafficking and effect on EGFR mutations in brain tumors after intravenous infusion of CART-EGFRvIII

(**A**) Comparison of CART-EGFRvIII quantification in brain tumor specimens compared to peripheral blood in each of the seven patients who underwent surgical resection at various time points (subject # and day # indicated on the *x* axis) after CART-EGFRvIII infusion. Ratio is calculated on the basis of copies per microgram of genomic DNA in cells. (**B**) Levels of expression of EGFRvIII as determined by NGS of purified genomic DNA in brain tumor specimens obtained before or after CART-EGFRvIII infusion. Subject numbers are indicated along the right, and each subject is color-coded for clarity. Where more than one sample was obtained and tested separately, points show the mean. Bar indicates *P* value between pre- and post-CART levels in paired specimens by the Wilcoxon matched-pairs signed-rank test. (**C**) EGFR amplification in brain tumor specimens obtained pre– and post–CART-EGFRvIII infusion from all tissue samples tested. Bar indicates *P* value between pre- and post-CART levels in paired specimens by the Wilcoxon matched-pairs signed-rank test. Subject numbers are indicated along the right, and each subject is color-coded for clarity. (**D**) TCRβ CDR3 deep sequencing analysis of T cells infiltrating brain tumor specimens obtained before and after CART-EGFRvIII and (**E**) in the matching infusion product and post-CART brain tumor–infiltrating lymphocytes in three subjects (205, 209, and 211). Unique TCR sequences in the pre-infusion tumor biopsy are shown in the green box along the *x* axis in (D) and in the infusion product in the green box along the *x* axis in (E). In (D)

and (E), these are compared with post-infusion tumor specimen clonotype repertoire shown in red along the y axis. Shared clonotypes are displayed in a blue box.
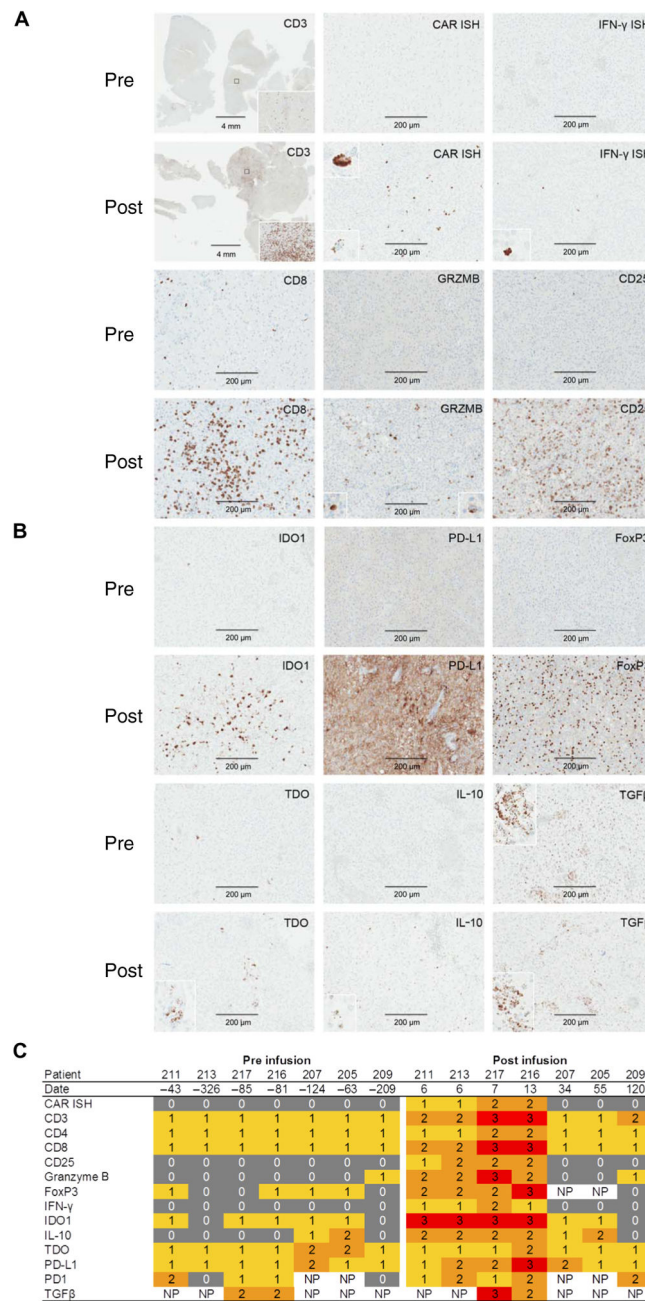
Fig. 5. Immunohistochemistry of the tumor microenvironment in GBM specimens before and after CART-EGFRvIII infusion

(**A**) T cell infiltration and phenotyping in pre– and post–CART-EGFRvIII infusion specimens from subject 216; pre-infusion specimens are from day −81, whereas post-infusion specimens are from day +13, relative to CART-EGFRvIII infusion at day 0. Top row shows low-power magnification of CD3 immunohistochemical stain, with high-power magnification as inset; ISH specifically for CAR sequences. T cell phenotyping is shown with ISH for IFN-γ and with immunohistochemistry for CD8, granzyme B (GRZMB), and the IL-2 receptor α chain (CD25). Scale bars, 4 mm (low-power graphs) and 200 μm (high-

power graphs). (**B**) In situ assessment of immunosuppressive molecules in the tumor microenvironment is shown before and after CART-EGFRvIII infusion in patient 216, including IDO1, PD-L1, FoxP3, TDO, IL-10, and TGFβ. (**C**) Summary table with heat map of T cell infiltration, CART-EGFRvIII trafficking, and tumor microenvironment in seven subjects before and after treatment with CART-EGFRvIII. NP, not performed; 0, not detectable. Date indicates day of specimen relative to CART-EGFRvIII infusion, which was designated as day 0.
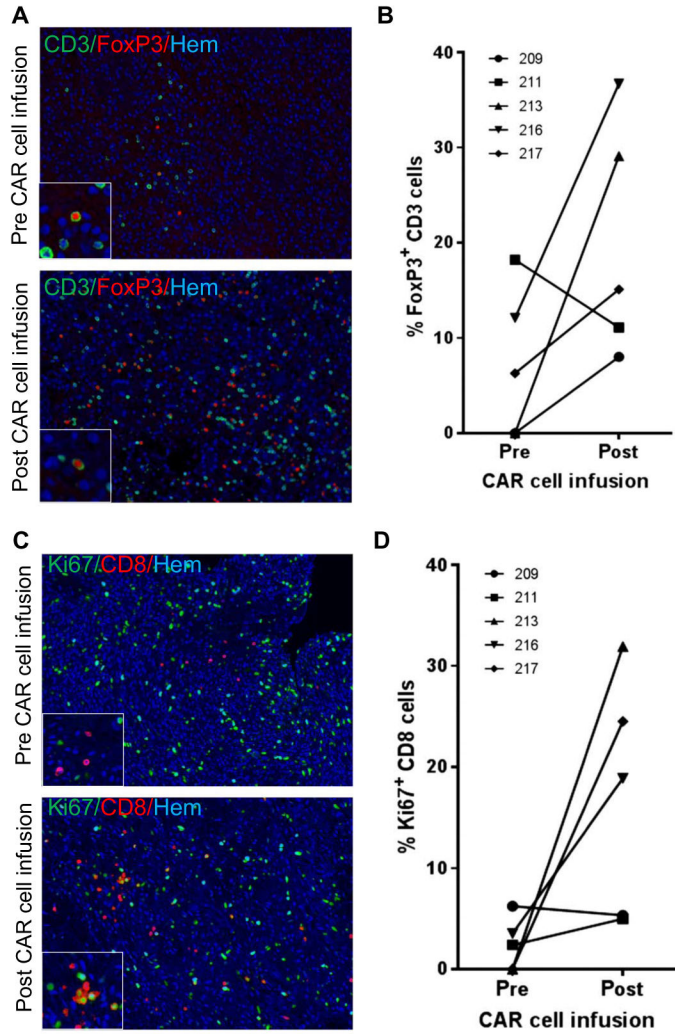
Fig. 6. Immunohistochemical colocalization of CD3/FoxP3 and CD8/Ki67
(**A** and **B**) Analysis of brain tumor samples performed pre– and post–CART-EGFRvIII infusion. Representative analysis of CD3/FoxP3 from patient 216 is shown in (A), with quantitative analysis of percent FoxP3+ CD3 cells shown for five subjects' brain tumor samples in (B). Two-tailed paired *t* test analysis did not demonstrate statistical significance (*P* = 0.10). Hem, hematoxylin. (**C**) Representative analysis of CD8/Ki67 staining in patient 213, and (**D**) quantitative analysis of percent Ki67+ CD8 cells for five subjects' brain tumor samples. Two-tailed paired *t* test analysis did not demonstrate statistical significance (*P* = 0.07).

Table 1

Patient and product characteristics.

	Median (*n* = 10)	Range
Age	59.5	45–76
Sex (male)	50%	
Time from initial diagnosis to infusion (in days)	358	179–682
Line of treatment at infusion		
2	20%	
3	40%	
4	40%	
Karnofsky performance status		
100	20%	
90	30%	
80	30%	
70	10%	
60	10%	
Receiving steroids at infusion	20%	
EGFRvIII expression	71%	(6–96%)
% T cells transduced	19.75%	(4.8–25.6%)
Dose of CART-EGFRvIII	5×10^8	$(1.75 \times 10^8 – 5 \times 10^8)$